INTERNATIONAL JOURNAL FOR NUMERICAL METHODS IN FLUIDS
Int. J. Numer. Meth. Fluids **31**: 275–283 (1999)

APPLICATION OF *h*-ADAPTATION FOR ENVIRONMENTAL FLUID FLOW AND SPECIES TRANSPORT

DARRELL W. PEPPER* AND DAVID B. CARRINGTON

Department of Mechanical Engineering, University of Nevada at Las Vegas, Las Vegas, NV 89154-4027, USA

SUMMARY

An adaptive finite element model has been developed for simulating environmental fluid flow and species transport. The model uses Petrov–Galerkin weighting for the advection terms, mass lumping, and a *h*-adapting scheme that refines and unrefines the mesh using velocity and species concentration gradients. The model is currently being used to calculate atmospheric wind fields over the Nevada Test Site, and to calculate groundwater transport in saturated or unsaturated porous media. The model runs on Pentium PCs and SGI workstations; a parallel version of the model runs on an SGI Origin 2000 computer. Copyright © 1999 John Wiley & Sons, Ltd.

KEY WORDS: environmental; finite element; atmospheric; groundwater; *h*-adaptation

1. INTRODUCTION

A finite element model that uses *h*-adaptation has been developed to calculate environmental fluid flow and species transport. By allowing the mesh to adapt during solution of the transient, non-linear equations of motion, accuracy can be significantly enhanced at reduced computational costs and less overall storage.

Adaptive techniques have typically been used to simulate compressible and incompressible flows, including complex flows involving turbulence and combustion processes with shock capture. Only recently have adaptive techniques been used in earnest for environmental phenomena, e.g. groundwater transport in porous media and atmospheric transport over complex terrain. It is particularly important when using adaptive mesh techniques to choose an appropriate error evaluator and ensure that mesh refinement and unrefinement occurs rapidly during transient solutions.

There are basically three types of adaptation now being utilized for solution of linear and non-linear transport equations: *r*-adaptation, *h*-adaptation and *p*-adaptation (see Zienkiewicz and Taylor [1]). In *r*-adaptation, a fixed, globally dense mesh is first established; as the solution progresses, the mesh is shifted (i.e. elements are distorted) and refined in those regions where most activity is occurring. The advantage of *r*-adaptation is that no new elements are needed in the overall mesh; the main disadvantage is that distorted elements lead to solution oscillations and divergence. In *h*-adaptation, the mesh becomes refined by adding new elements

* Correspondence to: Department of Mechanical Engineering, University of Nevada at Las Vegas, Las Vegas, NV 89154-4027, USA.

CCC 0271–2091/99/170275–09$17.50

to those regions where steep gradients are developing. The main advantage of h-adaptation is the ability to keep elements from becoming overly distorted; the principal disadvantages are the addition of new elements (increasing the size of the mesh), and the creation of 'virtual' (or 'hanging') nodes when using quadrilaterals. In p-adaptation, the order of the interpolation is enhanced, while keeping the mesh relatively coarse. The advantages of the p-method are the accuracy improvements and need to create only a very coarse mesh; the disadvantages are the complexity in creating such codes and the range of flow speeds [2]. Latest research efforts are aimed at combinations of h- and p-methods [3].

Incorporation of adaptive methods into commercial codes has only recently begun in earnest; however, a lot still needs to be done before such techniques can be used with ease and speed. A need now exists to develop more optimal techniques for h-adaptation in large problems—especially in environmental flows.

In this study, a finite element based h-adaptive algorithm is developed to calculate fluid flow and species transport in environmental problems, with particular emphasis on atmospheric wind field prediction and dispersion of particulates over irregular terrain, and groundwater transport in saturated and unsaturated porous media. The algorithm is currently being used to calculate winds over the Nevada Test Site, and groundwater flows at the Nevada Test Site and Yucca Mountain Repository Site in Nevada and the F-Area Basin at the Savannah River Site in Aiken, SC. Versions of the algorithm run on enhanced PCs, workstations and Cray class supercomputers, including an SGI Origin 2000 parallel computer.

2. GOVERNING EQUATIONS

2.1. Atmospheric motion and species transport

The Galerkin weighted residual method is used to discretize the atmospheric equations of motion and energy. The weak formulation yields the matrix equivalent forms of the governing equations, which can be written as [4]

$$[M]\{\dot{V}\} + ([K] + [A(V)])\{V\} + C^T\{p\} = \{F_V\}, \tag{1}$$

$$[M][\dot{\theta}] + ([K_\theta]) + [A(V)]\{\theta\} = \{F_\theta\}, \tag{2}$$

$$[M]\{\dot{q}\} + ([K_q] + [A(V)])\{q\} = \{F_q\}, \tag{3}$$

$$[M]\{\dot{\chi}\} + ([K_\chi] + [A(V)])\{\chi\} = \{F_\chi\}, \tag{4}$$

where V is the velocity vector (m s^{-1}), C^T is the gradient operator, θ is potential temperature (°C), q is specific humidity, and χ is species concentration (g m^{-3}). The matrix coefficients (denoted by [ ]) and column vectors ({ }) are integral relations based on the value of the shape function and its derivatives with respect to x, y and z. The dot above the variable refers to time dependence, and the caret denotes the trial approximation, e.g.

$$\hat{V}(x, y, z, t) = \sum N_i(x, y, z)V(t), \tag{5}$$

where N_i is the shape function. The matrix expressions are described in Pepper [5].

An explicit Euler scheme is used to advance the solution in time. Mass lumping is employed, along with reduced integration (in regions where the mesh is not distorted). In order to reduce numerical dispersion, a Petrov–Galerkin technique is used for the advection terms [6]. The use of this weighting function selectively eliminates the dispersive computational noise associated

with steep gradient resolution. Mesh adaptation accurately captures concentration fronts and resolves steep gradients as the solution progresses in time without requiring *global* remeshing of the problem domain.

Prior to solving the prognostic equations of atmospheric motion, an objective analysis scheme is used to produce a diagnostic wind field. Data from meteorological towers are employed to create a three-dimensional approximation. The surface wind field is constructed from measured data by interpolation to the initial mesh using inverse distance-squared weighting. Once the surface level flow field has been established, the upper level wind data are interpolated to the three-dimensional grids. A variational formulation (elliptic equation) is then solved for the potential and the velocities 'corrected' to ensure mass consistency [5,7]. This form of diagnostic analysis produces a realistic three-dimensional wind field, which is mass consistent and fairly accurate, and can be used to quickly generate trajectories of concentration resulting from accidental releases. The diagnostic wind field is used as input for the prognostic solution.

2.2. Groundwater flow and species transport

The governing equations for groundwater flow and subsurface transport of toxic material are quite different than those that describe atmospheric dispersion. In groundwater transport, the diffusion coefficients are more important in describing subsurface movement. Groundwater flow is quite slow, and is usually modeled with much simpler, linear forms of the equations of motion (compared with the non-linear equations describing atmospheric winds)—also, mass consistent 'wind fields' and 'velocity corrections' are not required. The transport of contaminant within soil layers, on the other hand, is more complicated than atmospheric dispersion. Hence, more time and effort is spent in solving the species equation.

The Galerkin procedures for solutions of the groundwater and species transport equations are analogous to those for atmospheric transport. The matrix equivalent forms of the governing equations for groundwater head and species transport [8,9] are

$$[M]\{\dot{h}\} + [D_h]\{h\} = \{F_h\}, \tag{6}$$

$$[M]\{\dot{\psi}\} + [D_\psi]\{\psi\} = \{F_\psi\}, \tag{7}$$

$$[M]\{\dot{\chi}\} + ([D_\chi] + [A(V)])\{\chi\} + \{F_\chi\}, \tag{8}$$

where h is head (m), ψ is pressure head (for unsaturated flows), χ is concentration ($\mathrm{g\,m^{-3}}$), V is the vector velocity field ($\mathrm{m\,day^{-1}}$), and D are the directionally dependent dispersion tensors ($\mathrm{m^2\,day^{-1}}$). Detailed descriptions of the matrix terms and governing equations are given in Pepper and Stephenson [10]. A Petrov–Galerkin scheme is likewise used to perturb the advection terms, and an explicit forward-in-time Euler scheme used to advance the solution in time.

3. *h*-ADAPTATION AND COMPUTATIONAL GEOMETRY

There are basically two types of unstructured meshes used in two-dimensional h-adaptation simulations—triangles and quadrilaterals; in three-dimensional cases, these become tetrahedrals and hexahedrals. The advantages of triangles lie with their ability to be easily generated and refined without creating 'virtual' (or 'hanging') nodes, i.e. mid-side nodes without connectivity to adjacent vertex element nodes. Quadrilaterals, while generally the preferred

type of element for fluid flow [1], create virtual nodes when refined that must be linked back to the corner nodes. This creates an element with one extra node on a face, and leads to a mesh compatibility problem, as shown in Figure 1(a) and (b). This is resolved using some programmatic bookkeeping; a more detailed discussion on the adaptation procedure is given in Pepper and Stephenson [10]. In this study, virtual nodes are used with quadrilaterals and hexahedrals during the mesh refinement cycle.

Algorithmic and combinatorial tools from computational geometry have been successfully applied for developing efficient mesh generation algorithms in recent years. The geometric approach looks promising for generating triangulations in two dimensions and tetrahedrization in three dimensions; similar efforts are underway on quadrangulation for quadrilaterals and hexahedrals. It may be noted that there can be exponentially many triangulations for a given set of input data points—one challenging problem is to select a suitable triangulation from exponentially many possibilities. Minimizing smallest angle, maximizing largest angle and reducing aspect ratio (ratio of major diameter to minor diameter of a triangle) are some of the widely used methods for measuring the quality of triangulation. Delaunay triangulation is known to have the property of simultaneously optimizing maxmin angle and minmax circumcircle. An example of Delaunay triangulation and quadrangulation is shown in Figure 2(a)–(c) for point selection based on meteorological tower locations within the Nevada Test Site [11].

4. RESULTS

4.1. Atmospheric flow

In the first example, mesh adaptation is used to model the transport of contaminant over two ridges [12]. The source ($S = 100$ g m^{-3} s^{-1}) is elevated 50 m above the surface. A uniform inflow boundary is assumed for the winds with $u = 5$ m s^{-1} along the left edge of the problem domain. The vertical extent is 600 m and the horizontal dimension is 2000 m. The height of the small ridge is 100 m and the large ridge is 300 m. The final mesh and concentration pattern are shown in Figure 3(a) and (b) for $t = 400$ s. The original mesh contained 220 elements and the final adapted mesh contained 884 elements. The concentration is transported into the valley between the two ridges where is begins to diffuse vertically; the concentration continues to be advected over the surface of the higher ridge. The adapted mesh shows those regions where the concentration gradient and activity are highest.

In the second example, atmospheric flow is modeled over the Nevada Test Site. The NTS is located in the southern part of Nevada, near Las Vegas (see Figure 4(a)). There are 15 operational towers located within the test site. An unstructured surface mesh, showing the

Figure 1. Virtual nodes for (a) two-dimensional quadrilateral and (b) three-dimensional hexahedral.

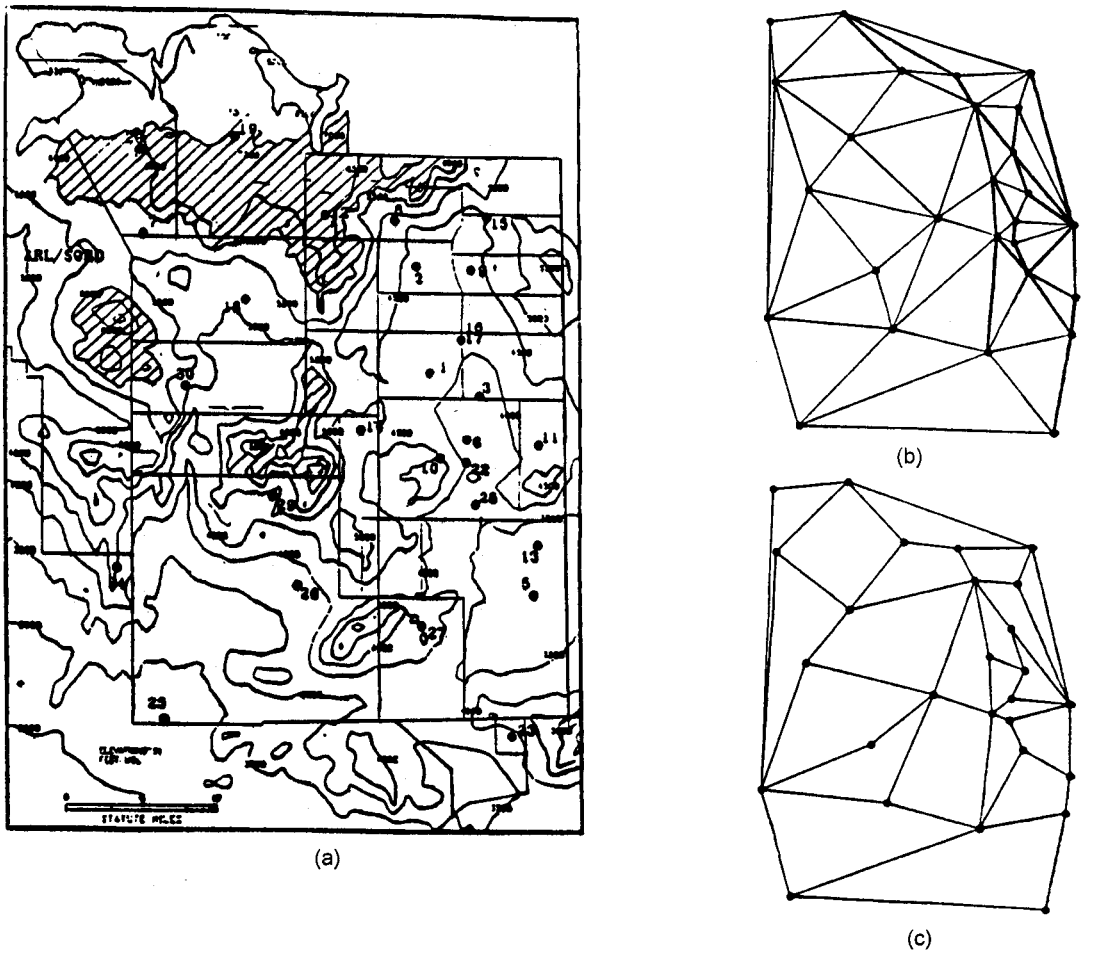

Figure 2. Meteorological towers for (a) Nevada Test Site, (b) mesh using Delaunay triangulation, and (c) mesh using Delaunay quadrangulation.

location of the towers, appears in Figure 4(b). A total of five layers were used to create the three-dimensional mesh over the site, with the second level at 10 m above the surface, the third level at 50 m, the fourth at 300 m, and the top level at 1000 m. Meteorological tower (10 m) and upper air data from 1 January, 1993, were used to initialize the wind field. Figure 4(c) and (d) show the wind patterns and topographic contours (gray shading), at the 10 m and 300 m levels.

4.2. Subsurface transport

The first example shows transient contaminant dispersion in saturated soil for a constant source ($S = 1$ g m^{-3}), as seen in Figure 5(a). The cross-section consists of two aquifers separated by a thin clay layer. The conductivities in aquifer 1 are $k_{xx} = 1.10$ (m day^{-1}), $k_{yy} = 6.0 \times 10^{-3}$; in the aquitard, $k_{xx} = 1.0 \times 10^{-7}$ and $k_{yy} = 6.0 \times 10^{-5}$. In aquifer 2, the conductivities are $k_{xx} = 1.20$ and $k_{yy} = 6.0 \times 10^{-5}$. These hydraulic conductivities are typical of the strata found at the Savannah River Site [10]. The initial mesh was created using 171

elements—the final mesh contained 684 elements. Concentration contours are shown after 2096 days. Several mesh refinements and unrefinements have occurred during the first 2000 days. The concentration is predominantly transported within aquifer 1 above the clay layer, with little vertical dispersion through the clay layer to aquifer 2. However, some of the contaminant has started to seep through the clay layer into aquifer 2 at around $x = 250$ m.

A cross-section of the proposed Yucca Mountain Repository Site for nuclear waste material is used for the second example [13], as shown in Figure 5(b). The soil is unsaturated, with very little annual rainfall. In this simulation, a water infiltration rate of 0.1 (mm per year) is assumed, with $k_{xx} = k_{yy} = 7.0 \times 10^{-4}$. Figure 5(b) shows a hypothetical release of contaminant from within the repository block. The transport and dispersion is non-linear, and takes many years to migrate through the soil. After 8000 years, the contaminant begins to reach the water table (bottom boundary) beneath Yucca Mountain.

5. PERFORMANCE

The algorithm was evaluated on three computer platforms: a Pentium 150 MHz PC with 80 MB RAM and 300 MB swap space, an SGI 02 with an R4000 chip, and an SGI Origin 2000 with ten CPUs. The test problem consisted of three-dimensional flow over a backward-facing step, and served as a simple example to evaluate speed and computational needs of the overall algorithm [15]. A fast Poisson solver is required for solving both atmospheric as well as groundwater problems. In atmospheric simulations, non-hydrostatic pressure is obtained from

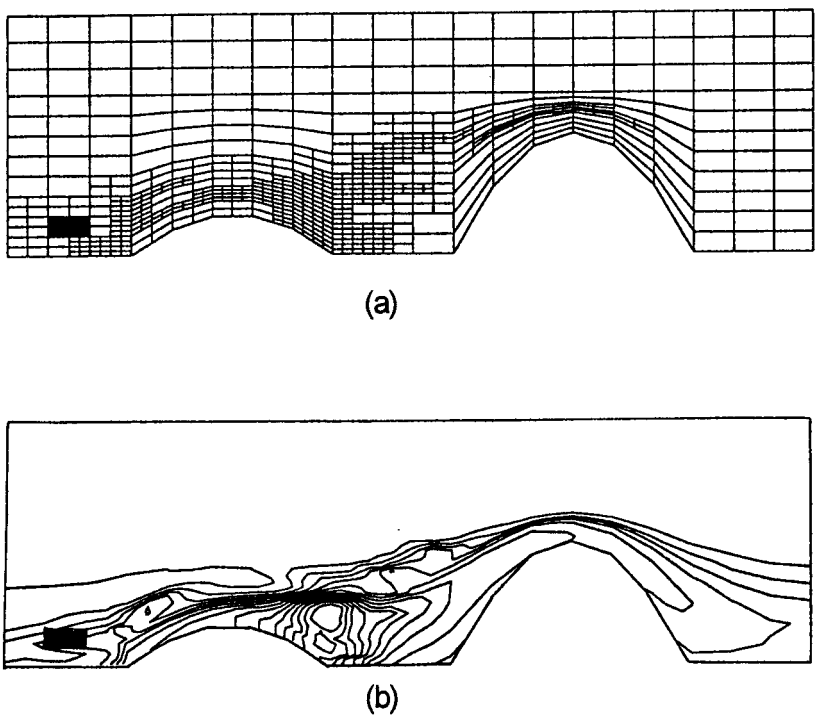

Figure 3. Atmospheric transport from an elevated source (a) adapted mesh and (b) isopleths.

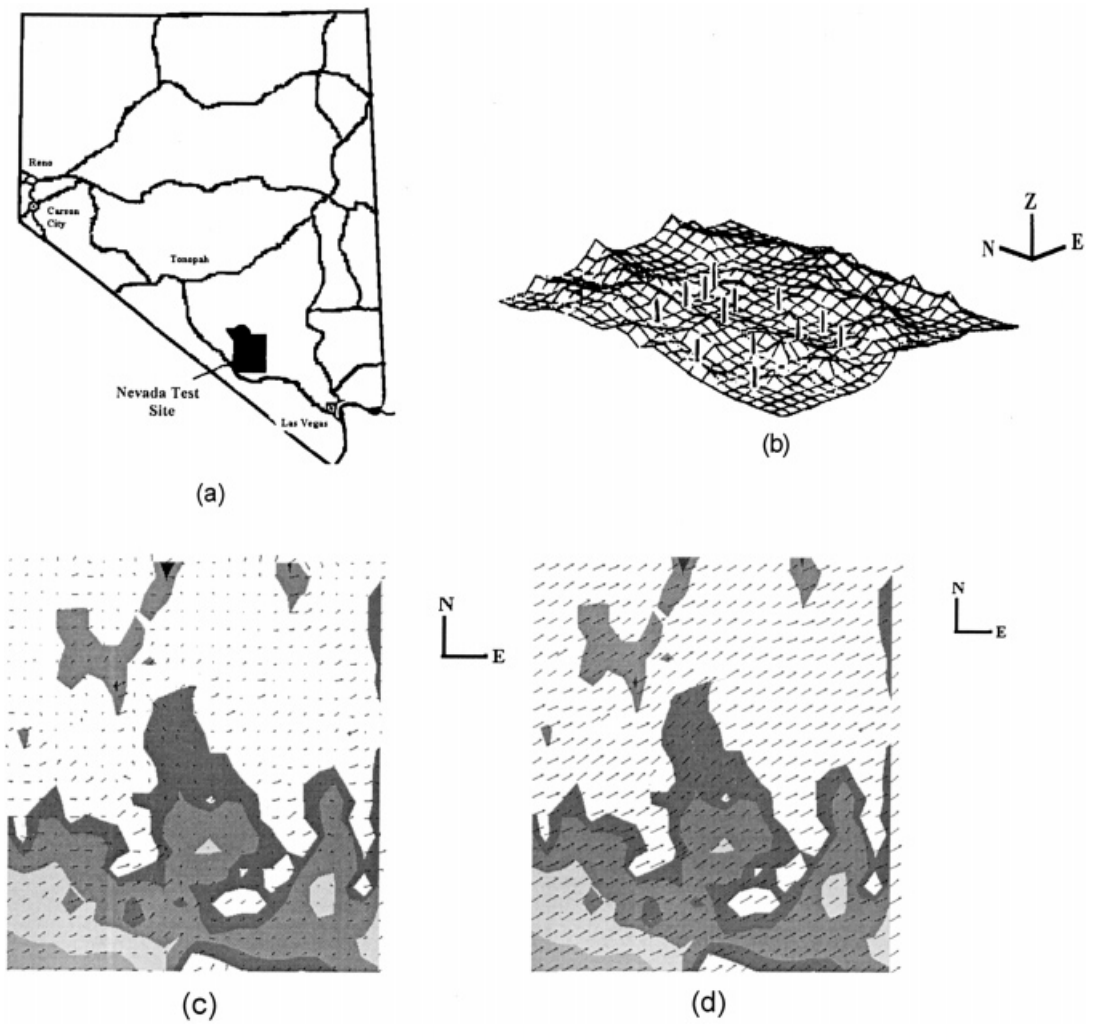

Figure 4. Wind fields over the Nevada Test Site for 1 January 1993 (a) the NTS, (b) towers within the NTS, (c) wind field at 10 m, and (d) wind field at 300 m.

solution of the elliptic equation for pressure, which arises from the non-linear equations of motion (Equation (1)). In groundwater flows, the Poisson equation for the pressure head (Equations (6) and (7)) is solved to provide velocities.

The majority of the overall computing time is spent generating converged solutions to the Poisson equations per time step. Either iterative or direct solvers are typically used for these equations. In this study, a Cholesky skyline solver was found to work best for the PC and workstation machines [16], and a block sparse Cholesky algorithm was used for the SGI Origin 2000 [17].

Overall, the origin was approximately nine times faster than the PC and workstation. Although the Pentium could handle problems on the order of 15000 nodes, the PC was incapable of solving finer meshes containing upwards of 30000 nodes; at higher mesh resolutions, the workstation has a distinct advantage over the PC in both storage and graphical

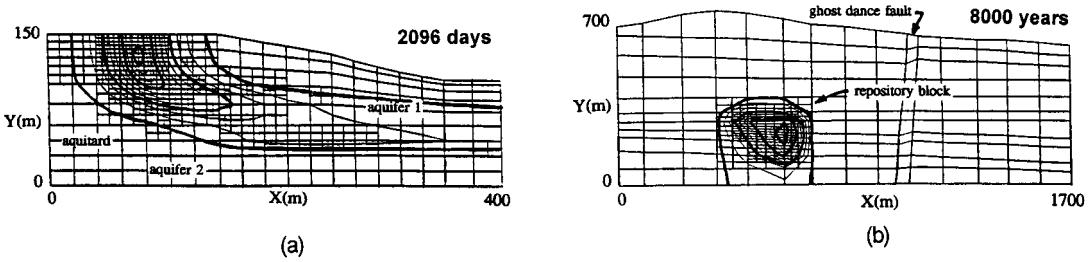

Figure 5. Groundwater flow and species transport (a) saturated flow and (b) unsaturated flow.

display capabilities. Running both fine (graded) and adapted meshes, the adapted mesh was about twice as dense in zones of high activity than the fine mesh, and produced twice the resolution. The solution speeds for the same number nodes on either a fine or adapted coarse mesh were nearly the same. Efforts are now underway to examine solution speeds using a parallel sparse conjugate gradient method.

6. CONCLUSIONS

A h-adaptive, finite element model has been developed for predicting velocities and species transport within complex environmental problem geometries. Coupling a h-adapting algorithm with a Petrov–Galerkin based finite element scheme produces very accurate solutions for environmental problems. The algorithm has been used to simulate groundwater transport and dispersion in saturated and unsaturated porous media, and used to generate three-dimensional wind fields over complex terrain. A two-dimensional code, written in C++, runs under WINDOWS utilizing a mouse and pull-down menus, and can be examined on the web; the web site is http://www.unlv.edu/Research_Centers/NCACM. The three-dimensional version, which also runs on enhanced PCs, is best run on workstation level computers to take advantage of the workstation's enhanced graphical display capabilities. A version of the three-dimensional algorithm has been optimized for running on an SGI Origin 2000 parallel computer [14]. The inclusion of p-adaptation with the h-adapting algorithm is under investigation.

REFERENCES

1. O.C. Zienkiewicz and R.L. Taylor, *The Finite Element Method*, *Vol. 2. Solid and Fluid Mechanics*, *Dynamics and Non-Linearity*, 4th edn., McGraw-Hill, London, 1991.
2. A.T. Patera, 'A spectral element method for fluid dynamics: laminar flow in a channel expansion', *J. Comput. Phys.*, **54**, 468 (1986).
3. J.T. Oden, T. Liszka and W. Wu, 'An h–p adaptive finite element method for incompressible viscous flows', *The Mathematics of Finite Elements and Applications VII*, Academic Press, New York, 1991, pp. 13–54.
4. P.A. Pielke, *Mesoscale Meteorological Modeling*, Academic Press, Orlando, FL, 1984.
5. D.W. Pepper, 'A 3D numerical model for predicting mesoscale windfields over Vandenberg Air Force Base', *Final Report*, *No. USAF/AFSC F04701-89-C-0051*, Advanced Projects Research Inc., Moorpark, CA, 1990.
6. C.-C. Yu and J.C. Heinrich, 'Petrov–Galerkin methods for the time-dependent convective transport equation', *Int. J. Numer. Methods Eng.*, **23**, 883–901 (1986).
7. C.A. Sherman, 'A mass-consistent model for wind fields over complex terrain', *J. Appl. Meteor.*, **17**, 312–319 (1978).
8. J. Bear, *Hydraulics of Groundwater*, McGraw-Hill, New York, 1979.
9. P.A. Domenico and F.W. Schwartz, *Physical and Chemical Hydrogeology*, Wiley, New York, 1990.

10. D.W. Pepper and D.E. Stephenson, 'An adaptive finite element model for calculating subsurface transport of contaminant', *Ground Water*, **33**, 486–496 (1995).
11. J. Bagga, L.P. Gewali and S. Ntafos, 'Visibility edges, mixed edges, and univue triangulation', *13th European Workshop on Computer Geometry*, Wurzburg, Germany, 1997.
12. D.W. Pepper and D.B. Carrington, 'A finite element model with *h*-adaptation for atmospheric transport of pollutants', in F.G. Garcia *et al.* (ed.), *Numerical Simulations in the Environmental and Earth Sciences*, Cambridge University Press, 1997, pp. 126–133.
13. D.W. Pepper and H.S. Sethi, 'An *h*-adaptive finite element model for subsurface contaminant transport', *9th Int. Conf. on Finite Elements in Fluids*, Venezia, Italy, 15–20 October, 1995.
14. D.W. Pepper, D.B. Carrington and J.M. Lombardo, 'A parallel *h*-adaptive finite element model for atmospheric transport prediction', *Adv. Eng. Software*, **29**, 2 (1998).
15. D.W. Pepper and D.B. Carrington, 'Convective heat transfer over a 3D backward-facing step', *ICHMT Int. Symp. on Advanced Computational Heat Transfer*, Cesme, Turkey, 26–30 May, 1997.
16. F.P. Brueckner and D.W. Pepper, 'Parallel finite element algorithm for three-dimensional inviscid and viscous flow', *AIAA J. Thermophy. Heat Transf.*, **9**, 240–246 (1995).
17. E. Ng and B.W. Peyton, 'Block sparse Cholesky algorithms on advanced uniprocessor computers', *SIAM J. Sci. Comput.*, **14**, 1034–1056 (1993).

